2013 IEEE/RSJ International Conference on
Intelligent Robots and Systems (IROS)
November 3-7, 2013. Tokyo, Japan

Obstacles Are Beneficial to Me! Scaffold-based Locomotion of a Snake-like Robot Using Decentralized Control

Takeshi Kano and Akio Ishiguro

Abstract— **Snakes are able to move effectively by using terrain irregularities as scaffolds against which they push their bodies. This locomotion is attractive from a robotic viewpoint because irregularities in the environment of conventional robots interfere with their operation. In a previous work, we proposed a decentralized control mechanism of the scaffold-based locomotion of snakes, which combined curvature derivative control with local pressure reflex. Here, we practically demonstrate how a snake-like robot utilizing the proposed control scheme moves effectively by pushing its body against pegs.**

I. INTRODUCTION

In spite of the simple one-dimensional structure of snakes, they are astoundingly adaptive and versatile in their real time movement through an unstructured environment. What is particularly surprising is that they actively utilize terrain irregularities and produce effective propulsive force by pushing their bodies against scaffolds as illustrated in Fig. 1 [1-4]. This locomotion is hereafter referred to as "scaffold-based locomotion." This locomotion has attracted particular attention in the field of robotics because it has various potential applications such as in search-and-rescue operations [5-9].

Whereas terrain irregularities often reduce the functionality of most conventional robots, they are beneficial to the scaffold-based locomotion of snakes. Hence, it is probable that an ingenious mechanism that is essentially different from those of conventional robots underlies scaffold-based locomotion. Biological studies have been conducted on snake locomotion to elucidate its mechanism, which have provided relevant data on the spatiotemporal dynamics of the body movement and muscular activities of snakes in various environments [2-4]. In the field of robotics, various types of snake-like robots that reproduce scaffold-based locomotion have been developed [5-9]. However, these robots can only adapt to a few environments; hence, the exact mechanism of scaffold-based locomotion remains unclear.

Autonomous decentralized control, in which the coordination of simple individual components yields nontrivial macroscopic behavior and functionalities, could be the key to understanding scaffold-based locomotion. Centralized control, which is commonly used for conventional robots, has a major disadvantage, namely that the computational resources required for the control increase considerably as the degrees of freedom of the robot body increases. Autonomous decentralized control is, however, expected to produce highly adaptive and resilient locomotion through the coordination of many body points, each of which has several degrees of freedom [10-12]. In fact, autonomous decentralized control mechanisms have been observed in several living organisms; for example, they are utilized by the biochemical oscillators found in true slime molds [13] and the central pattern generators (CPGs) of various animals [14-16].

T. Kano and A. Ishiguro are with the Research Institute of Electrical Communication, Tohoku University, 2-1-1 Katahira, Aoba-ku, Sendai 980-8577, Japan {tkano,ishiguro}@riec.tohoku.ac.jp

A. Ishiguro is also with the Japan Science and Technology Agency, CREST, Sanban-cho, Chiyoda-ku, Tokyo 102-0075, Japan

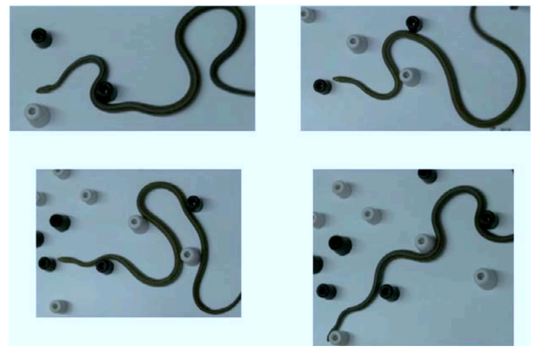

Fig. 1. Scaffold-based locomotion of a real snake (*Elaphe climacophora*).

We have thus far considered the mechanism of scaffold-based locomotion on the basis of curvature derivative control, which is an autonomous decentralized control scheme for generating a torque that is proportional to the curvature derivative of the body curve [17]. This control scheme was derived by a continuum-model-based theoretical analysis, wherein the spatial norm of the bending moment is minimized under the constraint of a fixed tangential acceleration of the body (see Appendix). Although this control scheme was derived from the perspective of locomotion efficiency, snake-like robots that utilize it exhibit adaptability in several environments. Hence, it is our consideration that this control scheme constitutes the basic propulsion mechanism of snakes and can be used as the key mechanism for achieving scaffold-based locomotion.

In our previous work, we proposed an autonomous decentralized control mechanism of scaffold-based locomotion, in which the curvature derivative control was combined with a simple reflexive mechanism. In this mechanism, the local pressure detected at a certain point in the body wall is fed back into the muscles on the contralateral side toward the head end [18,19]. Although we used simulations to show that the proposed control scheme worked well for scaffold-based locomotion, its validity is yet to be practically confirmed.

978-1-4673-6357-0/13/$31.00 ©2013 IEEE

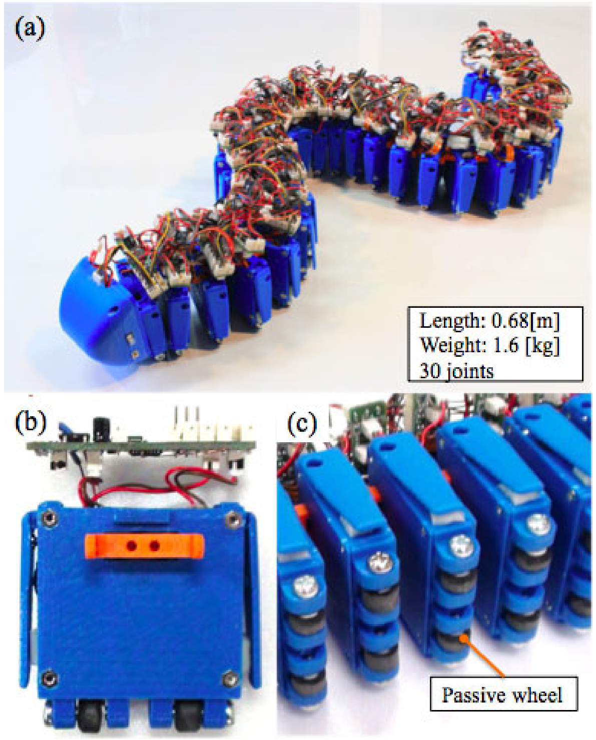

Fig. 2. The two-dimensional snake-like robot, HAUBOT III: (a) Overview, (b) body segment, and (c) underside of the robot.

We therefore developed the snake-like robot HAUBOT III (Hyper-redundant Adaptive Undulatory roBOTic system I II) to experimentally demonstrate how a robot using the proposed control scheme moves effectively by pushing its body against pegs.

The remainder of this paper is structured as follows. In Section II, we present the mechanical system of HAUBOT III and its autonomous decentralized control scheme. In Section III, the results of the experiments conducted using HAUBOT III are presented. Finally, we draw our conclusions and indicate the scope of future work in Section IV.

II. ROBOT

A. Mechanical System

Fig. 2 is a graphic overview of the developed robot HAUBOT III. The robot consists of 31 identical body segments that are concatenated one-dimensionally. The total length and weight of the robot are 0.68 m and 1.6 kg, respectively. Passive wheels are attached to the bottom of the segments to enforce anisotropy in the frictional coefficient between the body and the ground. The frictional coefficient in the normal direction was found to be 1.7 times that in the tangential direction, which agrees well with observations about real snakes [20].

Fig. 3 shows the detailed structure of each segment. Each segment is 14 mm (length) × 58 mm (width) × 54 mm (height) and has a servo motor, rotary potentiometer, control circuit with a microcomputer, and a battery. The servo motor

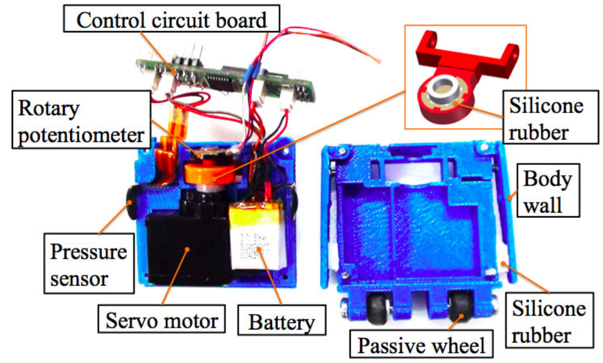

Fig. 3. Detailed structure of a segment.

is indirectly connected to the adjacent segment through a silicone rubber, which makes the system to work as a series elastic actuator [21]. Owing to this compliant mechanical structure, the joint can be passively bent to some extent, which enables the actual joint angle to deviate slightly from the motor angle. The joint angle is measured by the rotary potentiometer. A pressure sensor and silicone rubber are embedded on each side of a segment and covered by a body wall made from a hard material. When the body wall is pushed against external objects such as pegs, the sensor detects the corresponding pressure.

B. Control System

The design of the motor angle of each joint was based on our previously proposed autonomous decentralized control scheme [18,19]. However, a modification of the control scheme was inevitable for two reasons. Firstly, servo motors were used as actuators in the present robot, whereas antagonistic muscles were used as actuators in our previous model [18,19]. Secondly, experiments showed that body wave generated by curvature derivative control attenuates as it propagates from the head to the tail, which is apparently due to unexpected mechanical constraints. Hence, a modification of the curvature derivative control should be used to compensate for the effect of the attenuation.

Here, the motor angle of the ith joint $\bar{\phi}_i$ (the right direction is considered positive) is set as

$$\overline{\phi_i} = h + K_{s,i} \sum_{j=i+1}^{i+n_f} (f_{l,j} - f_{r,j}), \quad (1)$$

for $i \leq n_c$, and

$$\overline{\phi_i} = K_{d,i}\phi_{i-1} + K_{s,i} \sum_{j=i+1}^{i+n_f} (f_{l,j} - f_{r,j}). \quad (2)$$

for $i > n_c$. In the above equations, the value of h is given by the robot controller; n_c is the number of joints controlled by the robot controller; ϕ_{i-1} is the $i-1$th joint angle; $f_{l,j}$ and $f_{r,j}$ are the pressures detected on the left- and right-hand sides of the jth segment, respectively; n_f is the number of segments to which the local pressure is fed back; and $K_{d,i}$ and $K_{s,i}$ are positive constants. The first term on the right-hand side of

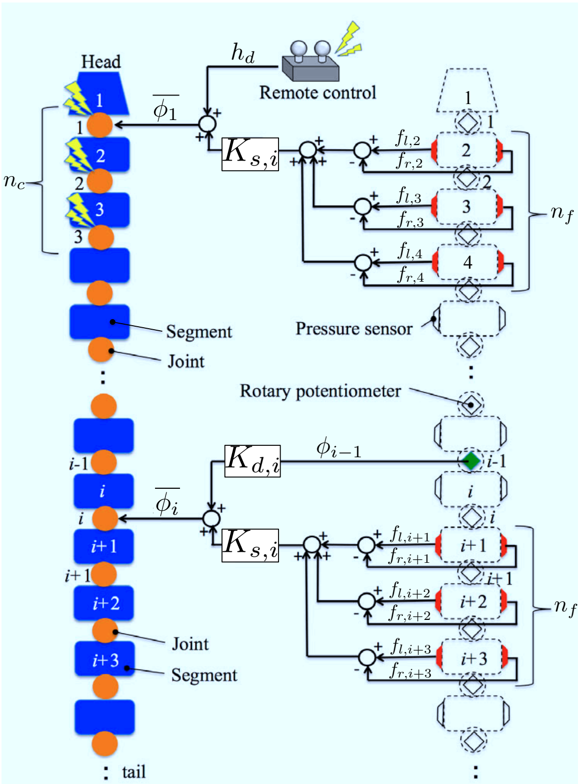

Fig. 4. Schematic of the control system. Both n_c and n_f are set to 3 in this figure.

(2) originates from the curvature derivative control, which was analytically derived using a continuum model [19] (see Appendix). This term forms the basic propulsion mechanism. The parameter $K_{d,i}$ has been introduced to compensate for the attenuation of the body wave. The term $K_{d,i}\phi_{i-1}$ corresponds to the curvature derivative control when $K_{d,i} = 1$ (see Appendix). However, $K_{d,i}$ has been set to be slightly greater than 1 so that the body wave appropriately propagates from the head to the tail. The second term on the right-hand side of (1) and (2) represents the local pressure reflex, which plays an essential role in scaffold-based locomotion. Whenever the body detects a local pressure on one side of a particular segment, the pressure reflex causes n_f joints at the head end to turn to the other side.

The proposed local reflexive mechanisms can be used to exploit scaffolds in the following manner. Suppose that the body makes contact with a peg near the inflection point of the body curve, as shown in Fig. 5(a), the curvature derivative control (red arrows) would cause torques to be generated at the joints near the contact point, thus pushing the body against the peg. The local pressure reflex then turns the joints at the head end of the contact point to the left (yellow arrows). This enables the head end of the body to push itself against the peg (Fig. 5(b)), thereby increasing the effect of the local pressure reflex. By this means, the robot uses the peg as a scaffold for effective movement.

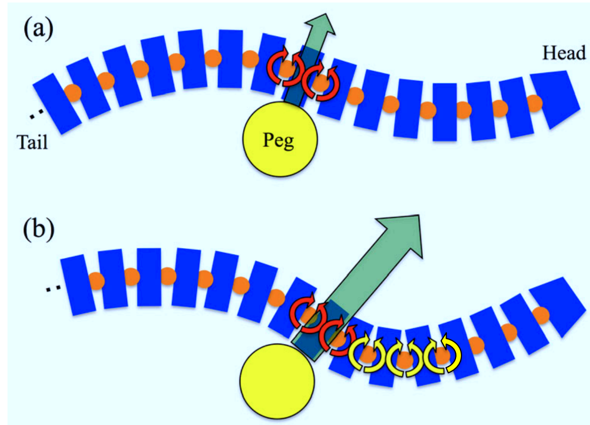

Fig. 5. Scaffold-based locomotion mechanism. The green arrows indicate the reaction force of the peg. The red and yellow arrows indicate the torques generated by the curvature derivative control and the local pressure reflex, respectively.

III. EXPERIMENTAL RESULTS

We conducted experiments using HAUBOT Ⅲ to investigate the practicality of the proposed control scheme. Experiments were first performed in an environment in which several column-shaped pegs, 60 mm in diameter and 20 mm in height, were placed randomly. In the initial condition, $\phi_i = 0$ for all i. The following parameter values were determined by trial and error:

$$n_f = 3;\ n_c = 1;$$
$$K_d = \begin{cases} 1.2 & (i \le 5), \\ 1.1 & (\text{otherwise}). \end{cases}$$
$$K_s = \begin{cases} 0.5 & (i \le 5), \\ 1.6 & (\text{otherwise}). \end{cases}$$

To increase the controllability of the robot, the values of K_d and K_s were respectively set to be greater and smaller for the first five segments than for the other segments. Through experiments, the proposed controlled scheme was compared with a scheme where only curvature derivative control is employed. Each experiment was repeated ten times. The trajectory of the robot was recorded by motion capture.

Fig. 6(a) shows photographs of the locomotion when the proposed control scheme was applied. We found that the robot moved by effectively pushing its body against the pegs. The trajectories (Fig. 7) show that each point along the body followed the path established by the head as in the motion of real snakes. We observed, however, that when only the curvature derivative control was implemented, the robot was unable to generate sufficient propulsion force and the locomotion velocity decreased significantly (Fig. 6(b) and Fig. 8).

We evaluated the locomotion efficiency using the following index E:

$$E = \frac{1}{D}\int_0^{t_0} P\mathrm{d}t, \tag{3}$$

where t_0 is the time taken by the robot to traverse the experimental field, P is the power consumed, and D is the distance travelled by the robot. The results are shown in Fig. 9. It is immediately apparent that E is smaller when the proposed control scheme is implemented than when the curvature derivative control is implemented. The results strongly suggest that the local pressure reflex plays a significant role in increasing the locomotion efficiency.

IV. CONCLUSION AND FUTURE WORKS

We focused on the locomotion of snakes in which terrain irregularities are used as scaffolds for effective movement. Although we previously proposed a decentralized control mechanism in which curvature derivative control was combined with local pressure reflex [18,19], it was not experimentally validated. Our newly developed snake-like robot was used for the practical demonstration of the proposed control scheme. The robot exploited terrain irregularities as scaffolds for effective locomotion.

Several problems, however, still remain. For example, the alignment of the pegs may cause the locomotion to collapse, and sophisticated skills are required to control the direction of the motion. The parameter values also need to be determined by trial and error, and the robot is incapable of three-dimensional motion. These problems make further

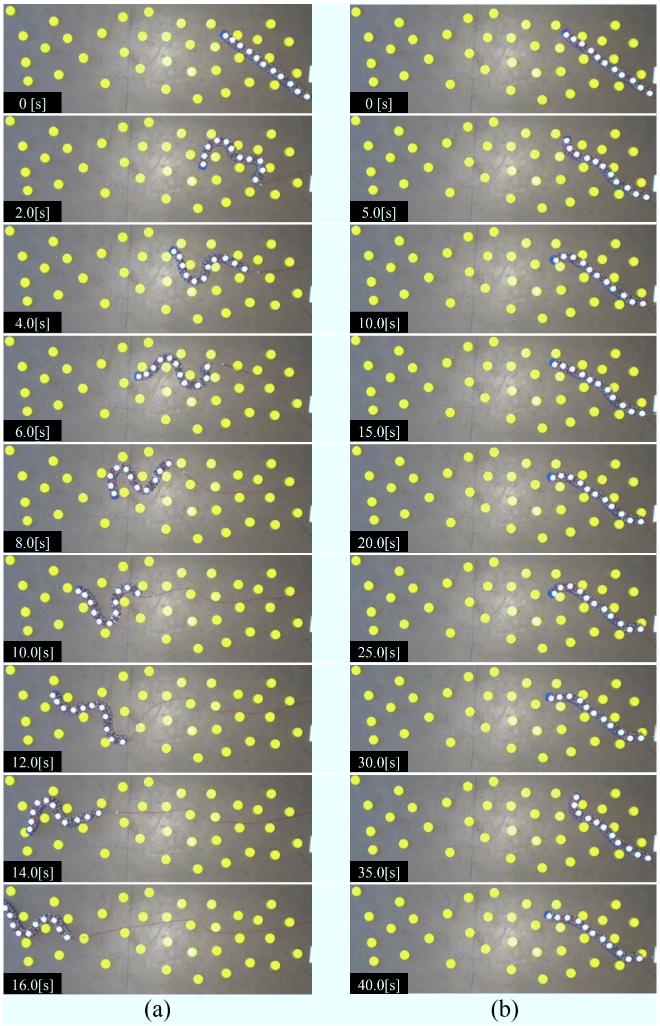

Fig. 6. Photographs of the locomotion of HAUBOT Ⅲ in an unstructured environment: (a) Using the proposed control scheme and (b) using only the curvature derivative control. The yellow dots are pegs, and reflectors were attached to the top of several segments to indicate the location of the robot.

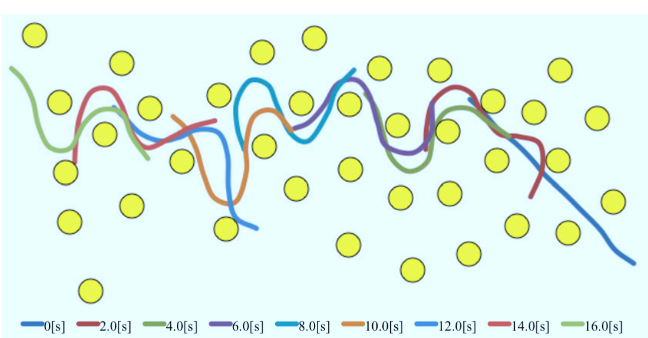

Fig. 7. Trajectory of the robot using the proposed control scheme. The colored curves indicate the position of the robot at intervals of 2.0 s, and the yellow dots indicate the pegs.

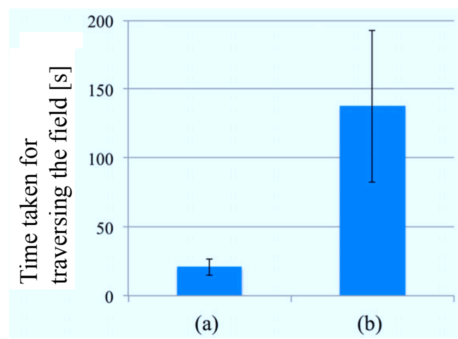

Fig. 8. Time taken by the robot to traverse the experimental field: (a) Using the proposed control scheme, (b) using only the curvature derivative control. The times shown are the mean values for ten trials, and the error bars indicate the standard deviations.

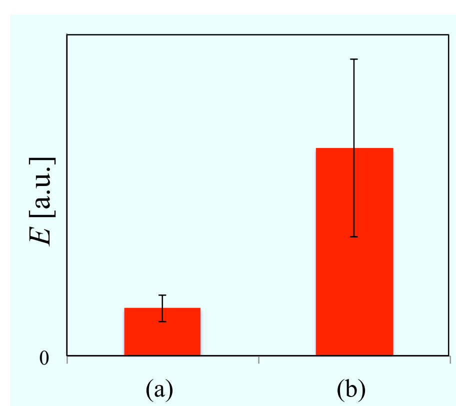

Fig. 9. Index of the locomotion efficiency E: (a) Using the proposed control scheme, (b) using only the curvature derivative control. The mean values for ten trials are shown, and the error bars indicate the standard deviations.

study necessary. We, however, believe that our present results would shed new light on the essential mechanism underlying animal locomotion and facilitate the development of robots that are highly adaptive like animals.

ACKNOLEDGEMENTS

This work was partly supported by the Grant-in-Aid for Young Scientists (B) No. 24760330 of the Ministry of Education, Culture, Sports, Science, and Technology (MEXT), Japan. The authors would like to express their gratitude for the cooperation of the late Dr. Michihisa Toriba, Dr. Atsushi Sakai, and Dr. Hisashi Miho of the Japan Snake Institute. The authors would like to thank Professor Ryo Kobayashi of the Graduate School of Hiroshima University for his helpful suggestion. The authors would also like to thank Dr. Takahide Sato of the Research Institute of Electrical Communication of Tohoku University for the development of the robot and the experiments.

REFERENCES

[1] J. Gray, The Mechanism of Locomotion in Snake, *J.Exp. Biol.*, vol.23, 1946, pp.101-120.

[2] J. Gray and H. W. Lissmann, The Kinetics of Locomotion of the Grass-snake. *J. Exp. Biol.*, vol. 26, 1950, pp. 354-367.

[3] B. C. Jayne, Muscular Mechanisms of Snake Locomotion: an Electromyographic Study of Lateral Undulation of the Florida Banded Water Snake (*Nerodia Fasciata*) and the Yellow Rat Snake (*Elaphe obsoleta*). *J. Morphol.*, vol. 197, 1998, pp. 159-181.

[4] B. R. Moon and C. Gans, Kinematics, Muscular Activity and Propulsion in Gopher Snakes, *J. Exp. Biol.*, vol. 201, 1998, pp. 2669-2684.

[5] S. Hirose, *Biologically Inspired Robots (Snake-like Locomotor and Manipulator)*, Oxford University Press, London, UK; 1993.

[6] P. Liljebäck, K. Y. Pettersen, Ø. Stavdahl, and J. T. Gravdahl, A Review on Modelling, Implementation, and Control of Snake Robots. *Robot. Auto. Sys.*, vol. 60, 2012, pp. 29-40.

[7] A. A. Transeth, R. I. Leine, C. Glocker, K. Y. Pettersen, and P. Liljebäck, Snake Robot Obstacle-aided Locomotion: Modeling, Simulations, and Experiments. *IEEE Trans. Robot.*, vol. 24, 2008, pp. 88-104.

[8] Z. Bayraktaroglu, A. Kilicarslan, A. Kuzucu, V. Hugel, and P. Blazevic, "Design and Control of Biologically Inspired Wheel-less Snake-like Robot,"*in Proc. of the First IEEE/RAS-EMBS International Conference on Biomedical Robotics and Biomechatronics*, 2006, pp. 1001-1006.

[9] P. Liljebäck, K. Y. Pettersen, and Ø. Stavdahl, Experimental Investigation of Obstacle-aided Locomotion with a Snake Robot. *IEEE Trans. Robot.*, vol. 27, 2011, pp. 792-800.

[10] T. Umedachi, K. Takeda, T. Nakagaki, R. Kobayashi, and A. Ishiguro, Fully Decentralized Control of a Soft-bodied Robot Inspired by True Slime Mold, *Biol. Cybern.*, vol. 102, 2010, pp. 261-269.

[11] T. Sato, T. Kano, and A. Ishiguro, On the Applicability of the Decentralized Control Mechanism Extracted from the True Slime Mold: a Robotic Case Study with a Serpentine Robot. *Bioinsp. Biomim.*, vol. 6, 2011, 026006.

[12] W. Watanabe, T. Kano, S. Suzuki, and A. Ishiguro, A Decentralized Control Scheme for Orchestrating Versatile Arm Movements in Ophiuroid Omnidirectional Locomotion. *J. Roy. Soc. Int.*, vol. 7, 2012, pp. 102-109.

[13] A. Takamatsu, R. Tanaka, H. Yamada, T. Nakagaki, T. Fujii, and I. Endo, Spatio-temporal Symmetry in Rings of Coupled Biological Oscillators of Physarum Plasmodium, *Phys. Rev. Lett.*, vol. 87, 2001, 078102.

[14] S. Grillner, O. Ekeberg, A. Manira, A. Lansner, D. Parker, J. Tegnér, and P. Wallén, Intrinsic Function of a Neuronal Network - A Vertebrate Central Pattern Generator, *Brain Res. Rev.*, vol. 26, 1998, pp. 184-197.

[15] A. A. V. Hill, M. A. Mashino, and R. L. Calabrese, Intersegmental Coordination of Rhythmic Motor Patterns, *J. Neurophysiol.*, vol. 90, 2003, pp. 531-538.

[16] A. J. Ijspeert, Central Pattern Generators for Locomotion Control in Animals and Robots: a Review. *Neural Networks*, vol. 21, 2008, pp. 642-653.

[17] H. Date and Y. Takita, "Adaptive Locomotion of a Snake Like Robot Based on Curvature Derivatives,"*in Proc. of the IEEE/RSJ International Conference on Intelligent Robots and Systems*, 2007, pp. 3554-3559.

[18] T. Kano, T. Sato, R. Kobayashi, and A. Ishiguro, Local Reflexive Mechanisms Essential for Snake's Scaffold-based Locomotion, *Bioinsp. Biomim.*, vol. 7, 2012, 046008.

[19] T. Sato, T. Kano, R. Kobayashi, and A. Ishiguro, "Snake-like Robot Driven by Decentralized Control Scheme for Scaffold-based Locomotion," *in Proc. of 2012 IEEE/RSJ International Conference on Intelligent Robots and Systems*, 2012, pp. 132-138.

[20] D. L. Hu, J. Nirodya, T.Scotta, and M. J. Shelleya, The Mechanics of Slithering Locomotion, *Proc. Nat. Acad. Sci. USA*, vol. 106, 2009, pp. 10081-10085.

[21] G. A. Pratt and M. M. Williamson, "Series Elastic Actuators", *in Proc. of the IEEE/RSJ International Conference on Intelligent Robots and Systems*, 1995, pp. 399-406.

APPENDIX

Date and Takita used a continuum model to analyze snake locomotion [17]. Although the continuum model was used to analyze three-dimensional locomotion, we here present a two-dimensional version of the model. In the continuum model, the backbone of the snake is represented by a smooth curve of zero thickness, parameterized by its arc length $s \in [0,L]$, where $s=0$ and $s=L$ respectively denote the head and tail ends. Hereafter, the derivative with respect to s is denoted by the prime symbol ($'$). The following conditions are assumed:

- The backbone is not stretchable.
- The lateral velocity is zero.
- There is no longitudinal friction.

Under these assumptions, the equation of motion of the entire body is given by

$$m\alpha = \int_0^L \kappa\tau' \mathrm{d}s, \tag{4}$$

where m is the total mass of the body, $\alpha \equiv \alpha(t)$ is the longitudinal acceleration, $\kappa \equiv \kappa(s,t)$ is the curvature, and $\tau \equiv \tau(s,t)$ is the actively generated bending moment. For a given value of α, the optimal bending moment that minimizes the quadratic cost function

$$J = \int_0^L \tau^2 \mathrm{d}s, \tag{5}$$

is derived using the Lagrange multiplier method as follows:

$$\tau^* = -\frac{m\alpha}{\displaystyle\int_0^L \kappa'^2 \mathrm{d}s} \cdot \kappa'. \tag{6}$$

This result can be approximated to a rigid link model by assigning $\kappa(s,t) \to \phi_i(t)$ and $-\kappa'(s,t) \to (\phi_{i-1}(t) - \phi_i)/\Delta l$, where $\phi_i(t)$ is the joint angle of the ith joint at time t and Δl is the link length. Then, the torque on the ith joint, $\tau_i(t)$, is given by

$$\tau_i(t) = K(\phi_{i-1}(t) - \phi_i(t)), \tag{7}$$

where K is the control gain that governs the longitudinal acceleration, which was used instead of $m\alpha/(\Delta l \int_0^L \kappa'^2 \mathrm{d}s)$ for simplicity. Equation (7) describes the proportional control of the ith joint, the reference of which is the $i-1$th joint angle. We note that, in our robot, the control equivalent of (7) can be achieved by making the motor angle $\bar{\phi}_i$ equal to ϕ_{i-1} (if attenuation of the body wave due to unexpected mechanical constraints is not considered). The control gain K can be tuned by changing the stiffness of the silicone rubber.